Interplay of Collective Excitations in Quantum Well Intersubband Resonances

Jianzhong Li* and C. Z. Ning†
Center for Nanotechnology, NASA Ames Research Center
Mail Stop N229-1, Moffett Field, California 94035-1000
(Dated: May 30, 2003)

Intersubband resonances in a semiconductor quantum well (QW) display some of the most fascinating features involving various collective excitations such as Fermi-edge singularity (FES) and intersubband plasmon (ISP). Using a density matrix approach, we treated many-body effects such as depolarization, vertex correction, and self-energy consistently for a two-subband system. We found a systematic change in resonance spectra from FES-dominated to ISP-dominated features, as QW width or electron density is varied. Such an interplay between FES and ISP significantly changes both line shape and peak position of the absorption spectrum. In particular, we found that a cancellation of FES and ISP undresses the resonant responses and recovers the single-particle features of absorption for semiconductors with a strong nonparabolicity such as InAs, leading to a dramatic broadening of the absorption spectrum.

PACS numbers: 78.67.De, 78.30.Fs,78.20.Bh,73.21.Fg

Intersubband resonances (ISBRs) in semiconductor quantum wells (QWs) are physical basis for some of the most important technological progresses in optoelectronics in the last decade, such as quantum cascade lasers and quantum well infrared photodetectors [1, 2]. At the same time, they also provide an ideal platform for studying fundamental many-body physics. From a single particle viewpoint, ISBRs correspond to dipole-allowed transitions between subbands. It is, however, known that intersubband absorption is strongly modified by various collective excitations, such as Fermi-edge singularity (FES) and intersubband plasmon (ISP). Such collective excitations as a result of Coulomb interaction have been investigated extensively for ISBRs [3–16]. The current understanding of many-body effects in ISBRs can be summarized as follows: Using the self-consistent field approach [17], ISBR oscillator strength was shown [5, 12] to "collapse" into a sharp collective mode, which is blueshifted relative to the free-carrier spectrum. This is known as the depolarization effect. In this mean-field approach, collective response of ISP is the *only* contribution. In contrast, both FES and ISP resulting from the Fock and Hartree interaction, respectively, can be modeled on the same footing by directly treating the vertex term. Both Green's function method [6, 7, 9–11] and density matrix formalism [13, 18] have been applied. It was shown [13] that the inclusion of vertex term leads to a red shift of the absorption peak from that of the mean-field theory. The spectrum peak is then between the free-carrier peak and the depolarization dominated peak, with the spectral shape being dominated by FES [13].

In this Letter, we show that such a picture is not entirely correct, or at least incomplete. Specifically, we show that depolarization does not necessarily collapse the otherwise broad spectrum induced by nonparabolicity to a sharp peak. Nor is the spectral shape always dominated by FES when the vertex term is included. Our results show a much more complete and complicated picture of spectral changes in ISBRs, depending on system parameters such as electron density, well width, and nonparabolicity of the band structure. The interplay of various many-body effects such as exchange self-energy (XSE), vertex correction, and depolarization leads to a complete sequence of spectral changes from FES- to ISP-dominated features. Particularly interesting is that, in the intermediate regime where the two collective excitations are comparable, their mutual cancellation restores the broad spectrum at high density for semiconductors with a strong nonparabolicity. In other words, the interplay of comparably strong FES and ISP effectively *undress* the ISBRs of the collective effects, recovering the single-particle (SP) characteristics of ISBRs. Such a complete picture of many-body effects in ISBRs not only enriches our understanding of basic physics, but also enables a more accurate prediction of the optical properties of QW devices for infrared applications.

Our approach is based on the density matrix theory [19, 20] which describes ISBRs in terms of the intersubband semiconductor-Bloch equations (ISBEs), in analogy to the SBEs for interband transitions [19]. Only two conduction subbands are considered in this work. The ISBEs, derived similarly as for interband SBEs [19, 20], are given as follows:

$$\frac{df_{l\boldsymbol{k}}}{dt} = (-1)^l \,\mathcal{I}m(2\Omega_{\boldsymbol{k}} p_{\boldsymbol{k}}) + \left.\frac{df_{l\boldsymbol{k}}}{dt}\right|_{inc}, \tag{1}$$

$$\frac{dp_{\boldsymbol{k}}}{dt} = \frac{1}{i\hbar}(\varepsilon_{2\boldsymbol{k}} - \varepsilon_{1\boldsymbol{k}})p_{\boldsymbol{k}} + i\Omega_{\boldsymbol{k}}(f_{1\boldsymbol{k}} - f_{2\boldsymbol{k}}) + \left.\frac{dp_{\boldsymbol{k}}}{dt}\right|_{inc} \tag{2}$$

where $\Omega_{\boldsymbol{k}} = [\boldsymbol{d_k} \cdot \boldsymbol{E}_\perp(t) - \varepsilon_{21\boldsymbol{k}}]/\hbar$. $f_{l\boldsymbol{k}}$ ($l = 1, 2$ for ground and first excited subbands, respectively) and $p_{\boldsymbol{k}}$ are distribution functions and intersubband polarization, respectively. $\boldsymbol{k}$ is the in-plane wavevector. The QW plane is normal to the $\hat{z}$ direction. $\boldsymbol{d_k}$ is the $\hat{z}$-component of the dipole matrix element. $\varepsilon_{l\boldsymbol{k}} = E^{(0)}_{l\boldsymbol{k}} + \varepsilon_{ll\boldsymbol{k}}$ consists of subband dispersion (the first term) and XSE (the second term). Furthermore, the subscript *inc* stands for electron-electron and electron-phonon scatterings [20, 21]. In the following, we assume the dephasing rate approximation ($dp_{\boldsymbol{k}}/dt|_{inc} = -\gamma_p p_{\boldsymbol{k}}$) and neglect the weak dispersion of dipole matrix element ($\boldsymbol{d}_{\boldsymbol{k}} = d\hat{z}$).

In the linear response regime, the subband populations follow the Fermi-Dirac distribution. A solution of Eq. (2) in the form of $p_{\boldsymbol{k}} = P_{\boldsymbol{k}} \exp(-i\omega t)$ for an incident TM field $\boldsymbol{E}_\perp(t) = E_0 \exp(-i\omega t)\hat{z}$ is sought under the rotating wave approximation. Equation (2) is then reduced to

$$[\hbar(\omega + i\gamma_p) - (\varepsilon_{2\boldsymbol{k}} - \varepsilon_{1\boldsymbol{k}})]\, P_{\boldsymbol{k}} = (dE_0 - \varepsilon_{21\boldsymbol{k}})(f_{2\boldsymbol{k}} - f_{1\boldsymbol{k}}) \ , \quad (3)$$

The XSE part of energy $\varepsilon_{l\boldsymbol{k}}$ and the local field correction $\varepsilon_{21\boldsymbol{k}}$ are given, respectively, by

$$\varepsilon_{11\boldsymbol{k}} = -\sum_{\boldsymbol{q}}{}' \left[V_{\boldsymbol{q}}^{1111} f_{1\boldsymbol{k}+\boldsymbol{q}} + V_{\boldsymbol{q}}^{1212} f_{2\boldsymbol{k}+\boldsymbol{q}}\right] , \quad (4)$$

$$\varepsilon_{22\boldsymbol{k}} = -\sum_{\boldsymbol{q}}{}' \left[V_{\boldsymbol{q}}^{2222} f_{2\boldsymbol{k}+\boldsymbol{q}} + V_{\boldsymbol{q}}^{2121} f_{1\boldsymbol{k}+\boldsymbol{q}}\right] , \quad (5)$$

$$\varepsilon_{21\boldsymbol{k}} = -\sum_{\boldsymbol{q}}{}' \left[V_{\boldsymbol{q}}^{2112} P_{\boldsymbol{k}+\boldsymbol{q}} + V_0^{2211} P_{\boldsymbol{q}}\right] , \quad (6)$$

where $\sum_{\boldsymbol{q}}'$ sums over non-zero $\boldsymbol{q}$'s. $V_{\boldsymbol{q}}^{n_1n_2n_3n_4}$'s are Coulomb matrix elements with the superscripts indicating subband indices (see [20]). We emphasize that the (static) single plasmon pole approximation is used only in screening the exchange interaction as a consequence of intrasubband dynamic correlation [19, 22]. $\varepsilon_{21\boldsymbol{k}}$ has two Coulomb sources: the vertex term with $\boldsymbol{q} \neq \boldsymbol{0}$ (first term) and the depolarization term with $\boldsymbol{q} = \boldsymbol{0}$ (second term). The vertex term reflect the *nonlocal* nature of exchange interaction, while the depolarization term causes a dynamic screening of the intersubband polarization. They are responsible for FES and ISP, respectively, and lead to a *dressing* of ISBRs. Whereas the vertex term is $\boldsymbol{k}$-dependent and couples all the $P_{\boldsymbol{k}}$'s, the depolarization term is $\boldsymbol{k}$-independent and proportional to the total polarization. It is therefore a bona fide local field correction in the sense of the Lorentz field. It is the interplay of these two terms that is the main focus of this Letter.

Optical susceptibility is defined by $\chi(\omega) \equiv P/\varepsilon_0 E_0$ with the total polarization $P = 2S/[(2\pi)^2\mathcal{V}] \int d\boldsymbol{k} d^* P_{\boldsymbol{k}}$. $\mathcal{V} = WS$, W is the QW width and S is a normalization area. Generally Eq. (3) needs to be solved numerically. But it is interesting to observe that an analytical expression for $\chi(\omega)$ can be obtained which allows us to gain considerable insights into various many-body effects in ISBRs. After some algebraic manipulation of Eq. (3), we obtain following formal solution for the susceptibility

$$\chi(\omega) = \mathcal{D}(\omega) \times \frac{1}{2\pi^2 W} \int d\boldsymbol{k} \chi_{\boldsymbol{k}}^{(0)}(\omega)\Gamma(\boldsymbol{k}, \omega) \ , \quad (7)$$

which contains three "factors". The first one is the $\boldsymbol{k}$-resolved SP susceptibility

$$\chi_{\boldsymbol{k}}^{(0)}(\omega) = \frac{(f_{1\boldsymbol{k}} - f_{2\boldsymbol{k}})d}{\varepsilon_{2\boldsymbol{k}} - \varepsilon_{1\boldsymbol{k}} - \hbar\omega - i\hbar\gamma_p} \ , \quad (8)$$

whereas the second is the vertex correction satisfying

$$\Gamma(\boldsymbol{k}, \omega) = 1 + \sum_{\boldsymbol{q}} V_{\boldsymbol{q}}^{2112} d^{-1} \chi_{\boldsymbol{k}+\boldsymbol{q}}^{(0)}(\omega)\Gamma(\boldsymbol{k} + \boldsymbol{q}, \omega) \ , \quad (9)$$

The third, $\boldsymbol{k}$-independent, is the depolarization factor:

$$\mathcal{D}(\omega) = \left[1 + \sum_{\boldsymbol{q}} V_0^{2211} d^{-1} \chi_{\boldsymbol{q}}^{(0)}(\omega)\Gamma(\boldsymbol{q}, \omega)\right]^{-1} . \quad (10)$$

The SP susceptibility contains the nonparabolicity effect that introduces inhomogeneous broadening as subband separation $E_{2\boldsymbol{k}}^{(0)} - E_{1\boldsymbol{k}}^{(0)}$ varies with $\boldsymbol{k}$. The XSE reduces the energies of occupied subbands and causes a blue shift of the SP response if only subband 1 is populated. The vertex factor is related to FES in metals or Mahan exciton in interband transitions in the presence of a degenerate electron gas (DEG) [13, 22]. In the case of ISBRs, the difference from the Mahan exciton is that a valence band hole in the Mahan exciton is replaced by an electron in subband 2. The effect arises from correlation of an electron in the upper subband with the entire degenerate Fermi sea of the lower subband and is therefore a form of collective excitation. The depolarization factor is associated with ISP, since the pole in $\mathcal{D}(\omega)$ defines the light-coupling ISP mode. The ISBR peak position, or the pole of $\chi(\omega)$, is then the result of competition of two types of poles: the FES pole and ISP pole. The effects of nonparabolicity and XSE are contained in both poles. The interplay of these factors determines the ISBRs: absorption peak frequency and line shape.

We now examine the ISBRs quantitatively by numerically solving Eq. (3) using matrix inversion. We assume two parabolic subbands given by $E_{1\boldsymbol{k}}^{(0)} = \hbar^2\boldsymbol{k}^2/2m_1$ and $E_{2\boldsymbol{k}}^{(0)} = E_{21}^{(0)} + \hbar^2\boldsymbol{k}^2/2m_2$, where $E_{21}^{(0)}$ is the subband edge separation. We note that self-consistent determination of subbands only lead to small quantitative changes [23] to subband separation. As in [13], we choose GaAs and InAs to represent semiconductors with weak and strong nonparabolicity as reflected in the following mass values: $m_1 = 0.069m_0$, $m_2 = 0.078m_0$ for GaAs and $m_1 = 0.027m_0$, $m_2 = 0.039m_0$ for InAs. m_0 is the free electron mass. We assume further that only subband 1 is populated.

Fig. 1 shows ISBR spectra for GaAs QWs with varying well widths. First we notice the blue shift induced by XSE in subband 1. The amount of blue shift decreases with increase in well width as we proceed from the bottom row to the top row, due to the weakening of the Coulomb interaction as well width increases. Furthermore the $\boldsymbol{k}$-dependence of XSE leads to extra line broadening as seen by comparing the dotted lines with dashed ones. Addition of vertex term to XSE significantly narrows the spectra (see long dashed lines), showing the features of FES. As QW becomes thinner, the peak position in FES case moves closer to the free-carrier case (dotted line), manifesting XSE and the vertex term cancel to a greater degree. Such a cancellation of XSE and vertex term can be easily seen by summing over $\boldsymbol{k}$ in Eq. (3). This is true for both interband and intersubband transitions in an ideal 2D case. For interband transitions, the opposite dispersions of conduction and valence bands leads to a $\boldsymbol{k}$-dependence of transition energy, such that equation for the total polarization P cannot be closed. Therefore many-body effects exist through the coupling of individual $P_{\boldsymbol{k}}$ equations. The situation is however different in the intersubband case, where the curvatures of the subbands have the same sign. The $\boldsymbol{k}$-dependence of transition energy becomes weaker in general and depends on the mass difference. For the ideal case of equal mass, the transition energy becomes $\boldsymbol{k}$-independent, such that the total polarization P equation is now closed. The exchange interaction completely drops from the P-equation. Many-body effects completely disappears if there were no depolarization effect. It was noted [13] that this situation is somewhat analogous to the Kohn's theorem. If nonparabolicity effect is small such as in the case of GaAs, then a large cancellation of XSE and vertex term is expected, leaving the absorption peak position (without depolarization) very close to the free-carrier one. As well width increases, XSE and vertex term cancel to a lesser degree. As a result, the ISBR peak moves toward red side and further away from the free-carrier peak. The sharp peak around the lower-frequency end (the Fermi edge) is a signature of the FES first studied by Mahan in the context of correlation between a hole and a DEG. The physical basis in both cases is the *nonlocal* exchange interaction which gives rise to this collective excitation.

Compared with interband case, there is an additional many-body effect for ISBRs, the depolarization effect which is connected to another form of collective excitation. It is well-known that the depolarization effect causes a blue shift. We have therefore two collective excitations that attract the peak position of a resonance to opposite directions and compete for its oscillation strength. Thus the resonance peak with full many-body effects (solid lines) settles between the FES peak (determined by the exchange interaction) and the ISP peak (determined by the Hartree interaction), as is evident in Fig. 1. As well width increases, the depolarization effect becomes more important so that the full result peak moves closer to the ISP peak (see the two middle rows). Eventually for rather wide wells, the curve with full many-body effects is almost identical to the ISP spectrum (see the top row). The ISBR spectrum for such a wide well is fully dominated by the depolarization effect. Thus we have shown a sequence of behavioral change of the resonance spectrum from a competitive regime (where both collective excitation is comparable) to the ISP-dominated regime (where the depolarization effect dominates over the excitonic effect). Another common feature of all the spectra in solid lines in Fig. 1 is that the spectral shape does not change much as the relative strength of the two collective excitations change with the well width. The line shape with full many-body effects is always narrower than the free-carrier one irrespective of the relative oscillator strength of the two collective excitations.

The situation changes drastically for strongly nonparabolic semiconductors such as InAs, for which absorption spectra are shown in Fig. 2. First the dif-

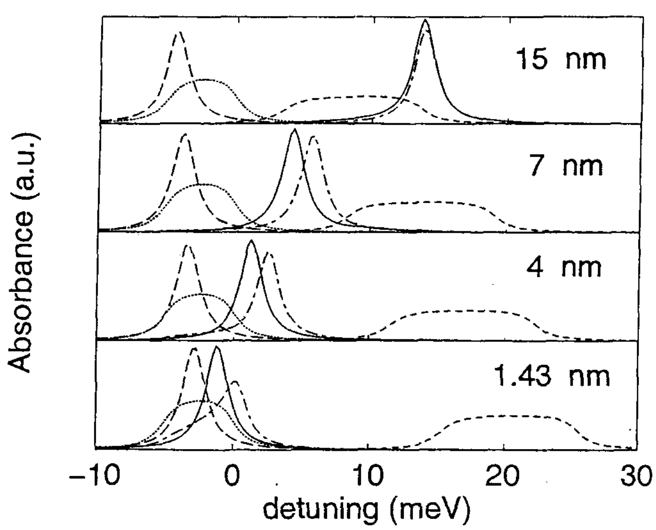

FIG. 1: Intersubband absorbance—$\mathrm{Im}[\chi(\omega)]$—for GaAs QWs with varying width as a function of detuning $\hbar\omega - E_{21}^{(0)}$. Electron density is 1.25×10^{12} cm^{-2}. Dotted lines: free-carrier; dashed lines: XSE; dot-dashed lines: ISP only; long dashed lines: FES; solid lines: full many-body effects.

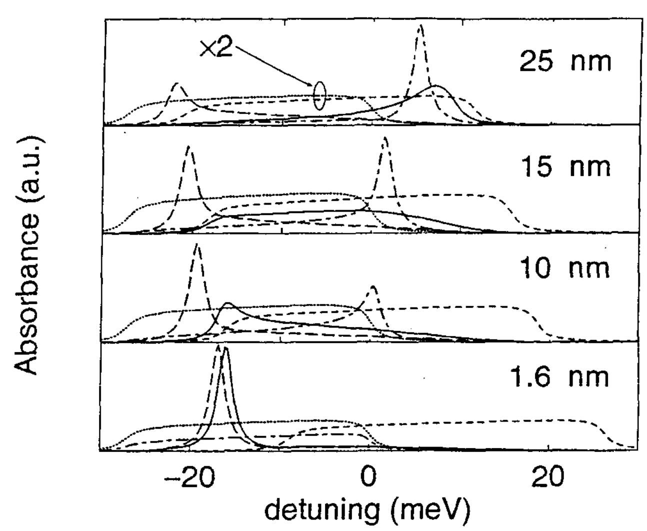

FIG. 2: Intersubband absorbance for different width InAs QWs. Electron density is 1.0×10^{12} cm^{-2}. Same line styles are used here as in Fig. 1. All dotted and dashed lines are multiplied by a factor of 2, as indicated in the top row.

ference between the free-carrier spectra and the ones with many-body effects becomes much greater for narrow wells than for GaAs. Without many-body effects, the spectra at high density become very broad due to nonparabolicity-induced inhomogeneous broadening. Second we see a complete sequence of spectral migration from FES-dominated (bottom row) to ISP-dominated spectrum (top row). Because of strong nonparabolicity, XSE and vertex term cancel to a much lesser degree. Consequently, FES feature is strongly enhanced for narrow wells (e.g., bottom row). Another striking difference from the case of weak nonparabolicity (cf. Fig. 1) is the change in spectral shape, as the relative strength of the two collective excitations changes with the well width. For the 15 nm QW, the comparable strengths of the two collective excitations lead to a near cancellation and leaves a rather broadened line shape. The spectral change from SP features to those dominated by collective excitations is described as *dressing*. It is interesting that the system is undressed in a parameter regime (in terms of well width and density) where one expects collective excitations are important. Indeed, individually both are important (see Fig. 2), but their interplay produces a seemingly undressed resonance—the SP picture is largely recovered. The strong nonparabolicity plays an important role here: it decreases the degree of cancellation between the XSE and vertex term, leaving a strong FES to compete with the ISP. On the contrary, weak nonparabolicity leads to a strong cancellation of the XSE and vertex term, making the ISP the stronger partner in the competition. Therefore such an undressing effect does not appear for GaAs QWs.

We also studied spectral change for both InAs and GaAs QWs at a fixed well width while varying electron density. At a low density, the full many-body absorption is almost identical to that of free-carrier case. With increasing density, the ISBRs are eventually dressed by the two collective excitations. As expected, the dominant excitation is ISP for very wide wells and FES for very narrow wells. The undressing effect is observed within a certain parameter window for strongly nonparabolic semiconductors.

In conclusion, we have systematically studied the effects of collective excitations on ISBRs. This was done by treating the Coulomb interaction in a consistent fashion. Such an investigation of spectral change with density and well width for two typical semiconductors uncovers a complicated and more complete picture of many-body physics in ISBRs. We showed significant change in spectral behavior such as line shape and peak position as a result of various many-body effects. In particular, the interplay of two comparably strong collective excitations leads to the undressing of both excitations, restoring single-particle features in the ISBR spectrum. Such a more complete picture not only enriches our understanding of many-body physics in ISBRs, but also allows a more accurate design of quantum structures for optoelectronic applications.

This work is supported by a DARPA-AFOSR grant and by a joint NASA-NCI program.

* Electronic address: jianzhng@nas.nasa.gov
† Electronic address: cning@mail.arc.nasa.gov; URL: http://www.nas.nasa.gov/~cning

[1] H. C. Liu and F. Capasso, eds., *Intersubband Transitions in Quantum Wells: Physics and Device Application I* (Academic Press, San Diego, 2000).
[2] K. K. Choi, *The Physics of Quantum Well Infrared Photodetectors* (World Scientific, River Edge, NJ, 1997).
[3] A. E. Ruckenstein, S. Schmitt-Rink, and R. C. Miller, Phys. Rev. Lett. **56**, 504 (1986).
[4] A. Pinczuk et al., Phys. Rev. Lett. **63**, 1633 (1989).
[5] M. Załużny, Phys. Rev. B **43**, 4511 (1991).
[6] J. C. Ryan, Phys. Rev. B **43**, 12406 (1991).
[7] S. L. Chuang et al., Phys. Rev. B **46**, 1897 (1992).
[8] D. Gammon et al., Phys. Rev. Lett. **68**, 1884 (1992).
[9] M. S.-C. Luo et al., Phys. Rev. B **48**, 11086 (1993).
[10] G. Gumbs, D. Huang, and J. P. Loehr, Phys. Rev. B **51**, 4321 (1995).
[11] D. Huang, G. Gumbs, and M. O. Manasreh, Phys. Rev. B **52**, 14126 (1995).
[12] R. J. Warburton et al., Phys. Rev. B **53**, 7903 (1996).
[13] D. E. Nikonov et al., Phys. Rev. Lett. **79**, 4633 (1997).
[14] R. J. Warburton et al., Phys. Rev. Lett. **80**, 2185 (1998).
[15] S. Tsujino et al., Phys. Rev. B **62**, 1560 (2000).
[16] J. B. Williams et al., Phys. Rev. Lett. **87**, 037401 (2001).
[17] T. Ando, A. B. Fowler, and F. Stern, Rev. Mod. Phys. **54**, 437 (1982).
[18] B. Nottelmann, V. M. Axt, and T. Kuhn, Physica B **272**, 234 (1999).
[19] H. Haug and S. W. Koch, *Theory of the Electrical and Optical Properties of Semiconductors* (World Scientific, Singapore, 1994).
[20] T. Kuhn, in *Theory of Transport Properties of Semiconductor Nanostructures*, edited by E. Schöll (Chapman & Hall, London, 1998).
[21] W. W. Chow and S. W. Koch, *Semiconductor-Laser Fundamentals* (Springer-Verlag, Berlin-Heidelberg, 1999).
[22] G. D. Mahan, *Many-Particle Physics* (Plenum Press, New York, 1981).
[23] J. Li et al., in *Progress in Semiconductors II: Electronic and Optoelectronic Applications*, edited by B. D. Weaver et al. (Materials Research Society, Warrendale, PA, 2003).